Quasiperiodic Energy Dependence of Exciton Relaxation Kinetics in the Sexithiophene Crystal

ARTICLE *in* THE JOURNAL OF PHYSICAL CHEMISTRY A · OCTOBER 2014

Impact Factor: 2.69 · DOI: 10.1021/jp506272b · Source: PubMed

2 AUTHORS:

Piotr Petelenz

Jagiellonian University

146 PUBLICATIONS **1,454** CITATIONS

SEE PROFILE

Emil Zak

University College London

7 PUBLICATIONS **6** CITATIONS

SEE PROFILE

THE JOURNAL OF PHYSICAL CHEMISTRY A

Article

pubs.acs.org/JPCA

Quasiperiodic Energy Dependence of Exciton Relaxation Kinetics in the Sexithiophene Crystal

Piotr Petelenz* and Emil Żak

K. Gumiński Department of Theoretical Chemistry, Faculty of Chemistry, Jagiellonian University, ul. Ingardena 3, 30-060 Krakow, Poland

ABSTRACT: Femtosecond kinetics of fluorescence rise in the sexithiophene crystal is studied on a microscopic model of intraband relaxation, where exciton energy is assumed to be dissipated by phonon-accompanied scattering, with the rates calculated earlier. The temporal evolution of the exciton population is described by a set of kinetic equations, solved numerically to yield the population buildup at the band bottom. Not only the time scale but also the shape of the rise curves is found to be unusually sensitive to excitation energy, exhibiting unique quasiperiodic dependence thereon, which is rationalized in terms of the underlying model. Further simulations demonstrate that the main conclusions are robust with respect to experimental factors such as finite temperature and inherent spectral broadening of the exciting pulse, while the calculated fluorescence rise times are found to be in excellent agreement with experimental data available to date. As the rise profiles are composed of a number of exponential contributions, which varies with excitation energy, the common practice of characterizing the population buildup in the emitting state by a single value of relaxation time turns out to be an oversimplification. New experiments giving further insight into the kinetics and mechanism of intraband exciton relaxation are suggested.

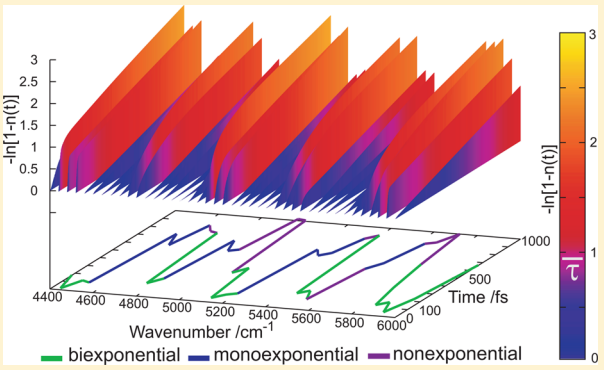

INTRODUCTION

In molecules, the dependence of the fluorescence lifetime on the excitation energy, indicative of complex relaxation kinetics, is uncommon but not exceptional.[1−3] In multicomponent, polydisperse, and/or disordered materials, such as polymers or aggregates,[4,5] it is rather commonplace and is often accompanied by nonexponential decay kinetics.[6,7] Normally, however, the dependence of decay kinetics on excitation energy (if any) is smooth and regular. To the best of our knowledge, the same usually applies to crystals.

In the present paper, we are dealing with the related process of fluorescence buildup upon femtosecond excitation. We argue that in the sexithiophene crystal (6T), this process is expected to be very sensitive to excitation energy, over a large energy interval exhibiting a seemingly irregular pattern of characteristic times and abruptly varying shapes of kinetic profiles. This kind of behavior is particularly unusual for a highly ordered, perfectly homogeneous system. While in the present paper sexithiophene is considered, the same mechanism is likely to be operative in a variety of similar cases.

In the crystal, the intense lowest electronic excitation of the sexithiophene molecule splits into four Davydov components, of which two are nominally allowed, and the absorption spectrum is dominated by the uppermost one.[8,9] The corresponding absorption band is asymmetric and broad due to the Fano-type coupling[10] of this Davydov component to the quasicontinuum of its own phonon replicas off the center of the exciton Brillouin zone.[11,12] The resultant diffuse absorption onset spreads down almost to the position of the lower Davydov component, covering the interval of 1.17 eV (according to experimental absorption spectrum[9]).

The system may be probed by optical excitation at any point of this interval; the progress of relaxation may be monitored by measuring the fluorescence buildup. Presumably, emission occurs from the lowest Davydov component (here identified with the bottom of the exciton band). The time scale of the relaxation process is on the order of hundreds of femtoseconds and, as experiments[13−15] demonstrate, strongly depends on the optical excitation energy.

The dependence is readily rationalized in terms of a simple model of exciton scattering with phonon release (cf. Figure 1). Owing to intensity lending from the discrete $\mathbf{k} = 0$ upper Davydov component,[16] the absorbed photon generates an unbound exciton−phonon pair (the two quasiparticles being endowed with opposite wave vectors); then, according to the tenets of the Fano approach,[10] the phonon is separated and dissipated within several femtoseconds. To reach the bottom of the exciton band, the remaining exciton sheds the surplus of its energy by scattering, thereby creating a hierarchy of secondary phonons, which are approximated as dispersionless[16] (Einstein model).

Received: June 24, 2014
Revised: September 3, 2014
Published: September 16, 2014

dx.doi.org/10.1021/jp506272b | J. Phys. Chem. A 2014, 118, 9653−9660

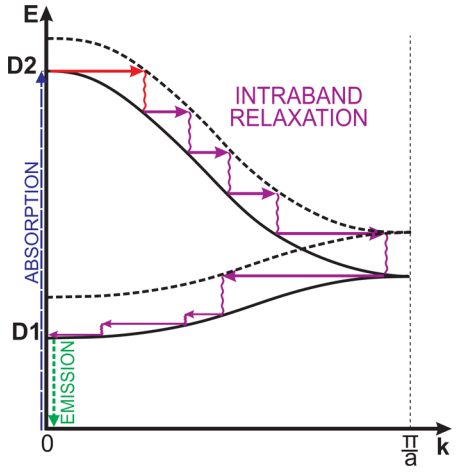

Figure 1. Schematic representation of absorption/emission/relaxation processes in the 6T crystal. The figure pertains to the exciton Brillouin zone and shows the exciton wave vector. In each scattering event, the excess quasimomentum is absorbed by the corresponding Einstein phonon, so that the total quasimomentum is conserved.

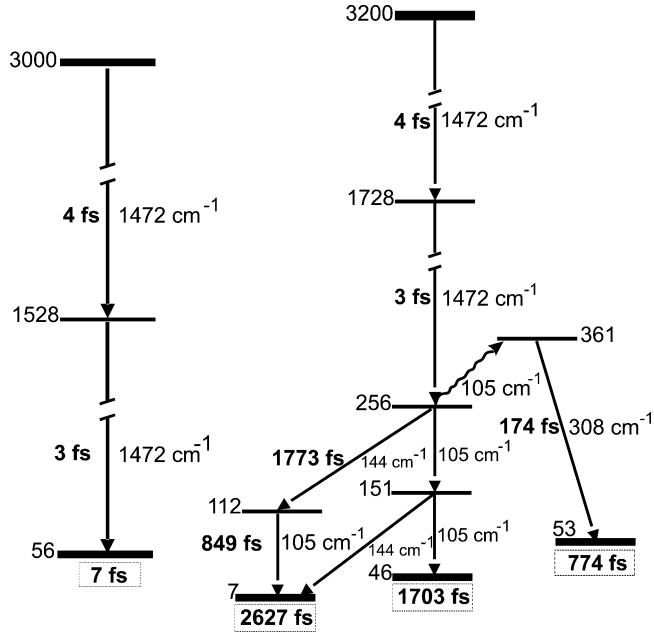

Figure 2. Schematic sequence of the leading relaxation processes for excitation energies 3000 and 3200 cm^{-1}. The indicated relaxation times are defined as the reciprocals of the corresponding transition rates calculated from the Fermi Golden Rule. The wavy line represents a thermally activated channel.

Here, the model of ref 16 and the rate constants calculated there are adopted to simulate the detailed form of the temporal dependence of population buildup at the bottom of the exciton band (measurable as fluorescence rise), following optical excitation at a specific energy. The calculations take into account all (six) intramolecular modes with substantial coupling constants (Huang–Rhys factors), known from quantum chemistry calculations.[17] The (previously ascertained[16]) dominant role of strongly coupled high-frequency modes in the relaxation process justifies the neglect of intermolecular vibrations. For the sake of simplicity, the four dispersion curves corresponding to the Davydov components are jointly treated as one continuous energy band with the width of 1.17 eV and a constant density of states[16] (for simplicity, only two of them are explicitly shown in the scheme of Figure 1). The exciton states with energies higher than the band bottom by less than one quantum of the lowest-frequency intramolecular mode (105 cm^{-1}) are assumed to be fully relaxed.

CALCULATIONS

Computational Scheme. Given the frequencies of the molecular vibrational modes[17] and the initial exciton energy (set by the energy of the absorbed photon), the ladder of consecutive exciton energy levels involved in the relaxation process (exemplified in Figure 2) is readily envisaged by considering all possible sequences of generated phonons.

Most of the levels thus deduced may decay in several ways, producing different phonons. The rate constants for these processes were earlier estimated based on the Fermi Golden Rule[16,18,19] from the respective vibronic coupling constants. These estimates have to be ameliorated in one respect; they were originally based on the simplified model with two molecules in the unit cell, directly applicable for the high-temperature (HT) phase of the 6T. However, most experiments were performed on the low-temperature (LT) phase, containing four molecules in the unit cell. Given the Davydov splitting (experimentally measured for the LT phase) and other relevant parameters being the same, this doubles the density of states, leading to doubled rate constants. While the previous values were accurate enough for order-of-magnitude estimates, they would not suffice for our present purposes and here have been modified accordingly.

The ultimate number of levels involved in the relaxation process depends on the initial excitation energy; near the absorption maximum at the top of the exciton band, it is on the order of 1000, yielding the same number of coupled rate equations. We have solved them numerically using the fourth-order Runge–Kutta algorithm, thereby obtaining the complete temporal dependence of the population flow. The experimentally observable fluorescence rise curve is identified with the population buildup $n(t)$ at the band bottom.

Depopulation of the band bottom by fluorescence, internal conversion to the ground state, and intersystem crossing has been consistently disregarded, being several orders of magnitude slower than the feeding processes.[20] We have repeated the calculations for different excitation energies, sampling the exciton band at 40 cm^{-1} mesh.

Global Evolution Descriptors. In our previous paper,[16] for each relaxation path defined by the sequence of created phonons, we characterized the rate of population buildup at the band bottom by specifying the hypothetical "total" relaxation time, approximated by the sum of the inverse rate constants for the consecutive steps of the relaxation process. In this way, we introduced the total time T for the *most probable* relaxation pathway (where at each step the most probable channel is selected) and the corresponding total time t for the *fastest* relaxation pathway (where at each step the fastest channel is selected). We expected the actual relaxation time to be bracketed between these two values.

Presently, the calculated population flow encompasses *all* of the pathways simultaneously. In this situation, as a consistent global descriptor of temporal fluorescence buildup, we introduce the effective rise time τ needed for 63% (i.e., $1 - e^{-1}$) of the initially generated population to reach the bottom of

dx.doi.org/10.1021/jp506272b | J. Phys. Chem. A 2014, 118, 9653–9660

the exciton band. This descriptor is crude but is expedient for analyzing the results, according to the common practice of characterizing the relaxation process by a single parameter. Its dependence on the initial excitation energy, obtained from the solutions of the rate equations, is depicted in Figure. 3 (colored

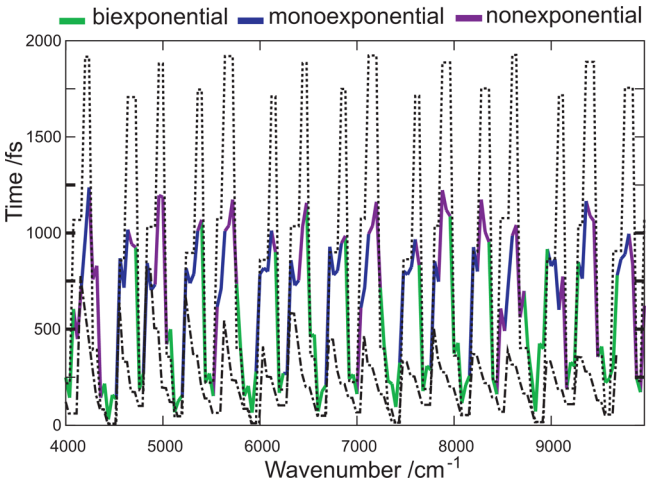

Figure 3. Calculated dependence of temporal relaxation descriptors on excitation energy (with respect to the bottom of the exciton band). Total relaxation times: for the most probable relaxation pathway (T, dotted line), for the fastest relaxation pathway (t, dash−dot line); the effective rise time was obtained by solving the rate equations (τ, continuous line, the colors encoding the type of anticipated fluorescence rise profile, vide infra).

line). For comparison, the two descriptors introduced previously (T and t) are represented by the dotted line and the dash−dot line, respectively. The figure shows that the effective rise time τ obtained from the solution of the full kinetic model is indeed usually bracketed between t and T, as anticipated.

To get further insight into the calculated kinetics, the individual fluorescence rise curves (corresponding to specific values of the excitation energy) have to be analyzed. Several examples of the temporal evolution of the population $n(t)$ at the bottom of the exciton band are shown in Figure 4, using the logarithmic scale that better visualizes the changes and allows one to extract individual exponential contributions. Evidently, the calculated fluorescence rise curves are not always representable by a single exponential. This suggests that the common practice of describing the relaxation process in

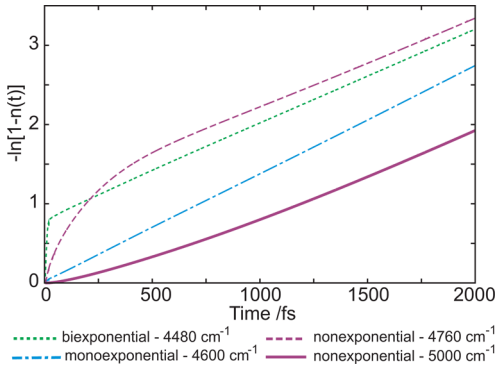

Figure 4. Typical examples of fluorescence rise curves (for several values of excitation energy).

sexithiophene by a single exponential and characterizing it by a single rise time[13−15] is a simplification and may potentially lead to interpretational errors.

The type of the rise profile (number of exponentials needed to reproduce it) is an independent and equally important global descriptor, which, as the plots demonstrate, in the system under consideration is expected to change erratically with excitation energy. When studied over a wider energy interval, it turns out to exhibit periodic energy dependence, as represented in Figure 3 by the color code. This feature seems to be rather unique. In general, a qualitative change of relaxation kinetics (embodied in the type of the rise/decay curve) with changing excitation energy seems to be a rare phenomenon, indicative of a transition from one relaxation mechanism to another. A sequence of such changes occurring at different excitation energies is still more peculiar. In the literature, we have found no example of such changes distributed periodically on the energy scale.

In most systems, temporal evolution accelerates with increasing excitation energy, which is a consequence of the increasing density of states. (The change may or may not lead to opening of new dissipation channels, qualitatively changing the overall kinetics.) In the 6T crystal, there is experimental evidence of a reverse effect, at least in some energy interval; for excitation at about 3.2 eV, the measured fluorescence rise time is on the order of 300−500 fs,[13,15] while excitation at 3.06 eV yields only about 120 fs.[14]

Rise Profile versus Relaxation Path. Our theoretical approach has a natural hierarchical structure. In an earlier paper,[16] without solving the kinetic equations (i.e., based on the "static" descriptors T and t) we identified the factors controlling the characteristics of individual relaxation pathways. We found, first, that the most probable paths are those engaging strongly coupled modes at the earliest stages of relaxation; the deeper into the relaxation process the strongly coupled modes continue to be involved, the larger the specific path's realization probability. Second, the total time of a given relaxation path is governed primarily by the value of the energy residue left after most of exciton energy is depleted by creation of phonons strongly coupled to the exciton. This allowed us to characterize some of the pathways as "fast" and others as "probable".[16]

Now, in an attempt to rationalize the unusual kinetics, we analyze the calculated exciton population flow, attributing the different types of rise curves to specific kinds of relaxation paths or combinations thereof. It should be mentioned in passing that the analysis might be easily extended to pinpoint specific bottleneck levels limiting the flow and determining the characteristic time of individual relaxation channels, but at the present (higher) hierarchical level, this kind of detailed information is not really needed.

Figure 3 shows that monoexponential curves (marked blue; dash−dot line in Figure 4), an experimentalist's standard, do not generally prevail. As follows from analysis of the population flow, the net rise time for such a curve is either governed primarily by one of the highly probable (but not very fast) pathways and slightly modified by other paths or alternatively unattributable to any dominant pathway but resulting from the averaging over many concurrent realizations of the relaxation process. In most cases, the pathways involved in this latter scenario are not very fast, engaging mostly medium-frequency modes (1073, 703, 308 cm^{-1}), characterized by moderately strong coupling to the exciton.

dx.doi.org/10.1021/jp506272b | J. Phys. Chem. A 2014, 118, 9653−9660

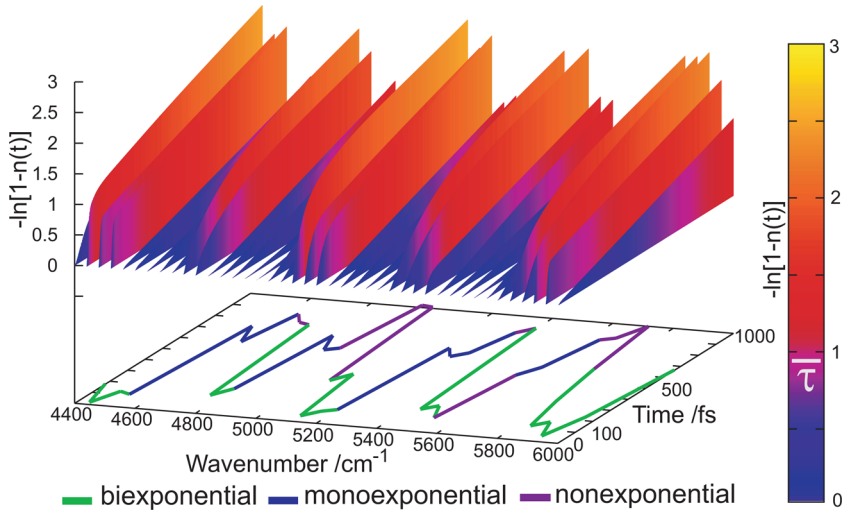

Figure 5. Dependence of the calculated fluorescence rise curve (on the logarithmic scale) on the excitation energy. The color on the rise profile encodes the fraction of the population that has reached the bottom of the exciton band by the specific time shown on the time axis. White indicator on the color-code scale: effective rise time τ. For each individual rise curve, the projection of the appropriate rise time τ onto the energy−time plane yields the corresponding fragment of Figure 3.

Biexponential curves (the corresponding fragments of the plot marked green in Figure 3, dotted line in Figure 4) occur whenever the energy surplus with respect to the bottom of the exciton band is a multiple of the vibrational quantum in the most strongly coupled 1472 cm^{-1} intramolecular mode, possibly accompanied by a quantum of somewhat less strongly coupled 703 or 1073 cm^{-1} vibration. In these cases, the dominant relaxation process progresses very quickly because the most probable relaxation path is also the fastest and, once entered, is rapidly (within several tens of femtoseconds) completed, later providing a steady population at the band bottom. Against this steady background, the (much smaller) contribution from a less probable and slower decay pathway, forking off at an early stage by engaging a slightly less active mode (or modes), is readily discernible. The two straight-line intervals of the dotted curve in Figure 4 correspond to the two stages of relaxation, resulting from the two decay branches.

The most complex situation (magenta in Figure 3, solid and dashed lines in Figure 4) emerges when the energy is slightly lower or higher than that in the preceding example, so that the rate of the first stage is reduced and approaches the rate of the second stage. Then, the two processes concomitantly contribute from the outset, with dominance tipping gradually from one branch to the other. The former two straight lines are no longer discernible, smoothly fusing into a superposition representing a nonexponential curve. Alternatively, this kind of nonexponential kinetics ensues when several competitive slow channels, forking off at different stages of the relaxation process, are characterized by comparable yet perceptibly different rates. In that case, the individual (possibly exponential) contributions from different pathways cannot be resolved, and the net kinetic behavior is nonexponential. This scenario often involves a bottleneck state located low above the band bottom, depopulated only by weakly coupled low-frequency vibrations (144, 105 cm^{-1}), which explains the long duration of the process.

Energy Dependence of Fluorescence Rise Curves. In Figure 5, the shapes of the rise curves are explicitly shown for a part of the energy spectrum. They are strikingly diverse, yet some features are more or less general. First, the shapes of the rise profiles follow the global descriptors in exhibiting quasiperiodic dependence on excitation energy. Second, in the long-time limit, the kinetics is always slow, being dominated by the bottlenecks mentioned above. Third, there is some correlation between the number of contributing exponentials and the overall pace of the relaxation process.

Namely, fast runs, with steep initial rise, are biexponential as a rule. They occur exclusively in the narrow energy intervals where the most probable relaxation path is also the fastest. In these cases, the nominal effective rise time τ is short but is generally too simplified a descriptor to characterize the kinetics. The purple coloration representing small population at the band bottom disappears so rapidly that it is barely perceptible, and the (much slower) asymptotic behavior is reached very early. This implies that the contribution from slow relaxation pathways, appearing at terminal stages of temporal evolution, is discernible only when most of the population has reached the band bottom. Consequently, in short time-span experiments or when the experimental noise is large, the slower long-time evolution may readily escape attention, and special caution must probably be exercised to notice it (vide infra). In contrast, it is also conceivable that an inherently slow experimental setup may entirely miss the rapid initial phase of relaxation, averaging the buildup of the fluorescing population over a time comparable with its own intrinsic time constant.

For most excitation energies, though, the initial population buildup at the band bottom is more sedate (the dark coloring continuing for a long time), which makes the shape differences between the rise curves visually less perceptible. Many of the profiles only slightly deviate from a single exponential, so that τ remains a reasonable descriptor, yet for some others (e.g., at about 4800 cm^{-1}, cf. also Figure 4), no adequate description in terms of exponential curves seems to be feasible.

As follows from the above observations, the quasiperiodic energy dependence of the relaxation profile shape is governed by the relation between the actual surplus of energy to be dissipated and the frequencies of the modes that are most strongly coupled to the exciton, just as noted for the relaxation time. The main pattern is set by the dominant 1472 cm^{-1} vibrational quantum, to be followed by the less strongly

dx.doi.org/10.1021/jp506272b | J. Phys. Chem. A 2014, 118, 9653−9660

coupled 703 and 308 cm^{-1} modes. The fact that the dependence is quasiperiodic but not exactly periodic is a consequence of the near-coincidences of the features due to these three frequencies that are not commensurate and to some marginal modulation due to the 1073 cm^{-1} mode.

The switching from one regime to another occurs within the excitation energy intervals on the order of 150−200 cm^{-1}, that is, very abruptly. In an actual experiment, this abruptness is blunted to some extent on account of the Heisenberg uncertainty principle stipulating that the short duration of the exciting light pulse must result in its increased spectral width, covering several mesh points of the plot, and by temperature broadening, not included in the above simulations.

SIMULATION OF EXPERIMENTAL CONDITIONS

Spectral Width of the Exciting Pulse. As a real exciting pulse has a finite temporal duration Δt, it also has a finite spectral spread $\Delta\omega$. The two widths (fwhm) are related by the expression $\Delta t\Delta\omega \geq \delta$ (ref 21), where δ is a constant ranging from about 1 to about 3, depending on the pulse shape. For example, in the experiment of Loi et al. (ref 14, vide infra), the cross correlation fwhm of 200 fs between the gate pulse and its second harmonic (used to excite the crystal) implies the spectral width in the range of 60−80 cm^{-1} for the exciting light intensity (assuming the two most common shapes, i.e., Gaussian and $sech^2$). The actual width, being compounded by equipment factors, may be larger than the above value, limited by the Fourier transformation.

Figure 6 shows the dependence of the effective rise time τ on energy, calculated for several spectral widths of the (Gaussian)

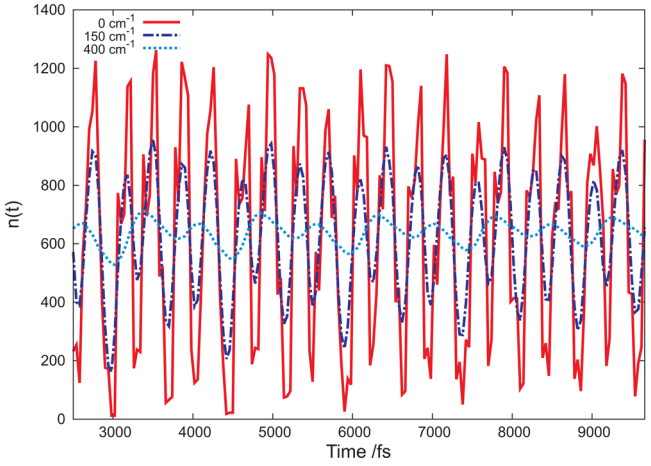

Figure 6. Relaxation time as a function of the excitation energy at zero temperature calculated for different spectral widths of the exciting pulse.

exciting pulse, corresponding (for Fourier-transform-limited pulses) to temporal durations ranging from 35 fs to infinity. As expected, for an energy-broadened pulse, the amplitude of the rise time changes is reduced because the wings of a pulse centered at a given "nominal" energy generate excitons also at nearby energies, for which the relaxation channels are different, leading to differing relaxation times. The net fluorescence rise time is an average of these contributions, weighted by the intensity of the exciting pulse at different energies, according to the spectral profile of the pulse. In effect, the energy-dependent variations in the effective fluorescence rise time are curbed but for reasonable pulse durations are still quite substantial, and the quasiperiodic energy dependence is preserved.

Temperature Dependence. All graphs presented above show the relaxation at zero temperature. At higher temperatures, the general pattern is not significantly affected, but (as follows from population flow analysis) the slowest relaxation pathways are accelerated owing to the opening of new (thermally activated) channels that draw from the population of bottleneck states close to the exciton band bottom. The probability of such activation is governed by the Boltzmann factor.

The results are displayed in Figure 7. For instance, for excitation at 3200 cm^{-1} (with respect to the bottom of the

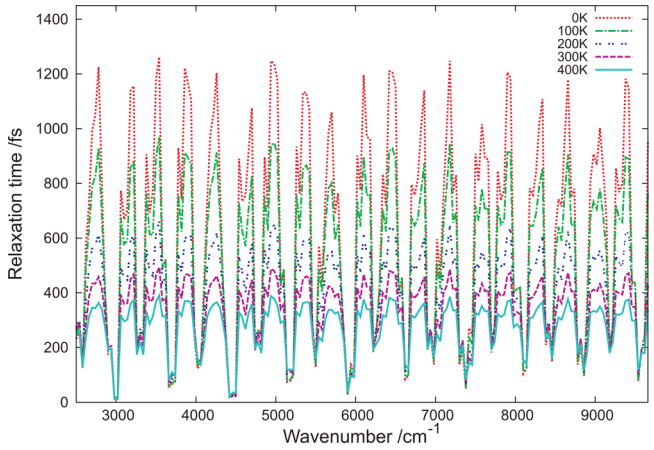

Figure 7. Relaxation time as a function of excitation energy at different temperatures ($\Delta\omega$ = 0).

exciton band), the relaxation time is expected to decrease from 1200 to about 350 fs upon temperature elevation from 0 to 400 K. The scenario is readily rationalized by analyzing the population flow. At 0 K, relaxation progress is limited by the long-lived bottleneck level at 256 cm^{-1}, from which thermal activation to the level at 361 cm^{-1} becomes feasible at higher temperatures, and the energy of this level is sufficient to enable fast relaxation by release of the quantum of the 308 cm^{-1} mode, relatively strongly coupled (cf. Figure 2, right panel).

In contrast, the fast relaxation paths tend to slow down at higher temperature because (owing to thermal activation of otherwise barely populated levels) a part of the population strays away from the most effective routes, getting distributed over a random set of less favorable channels. However, this effect is less pronounced because the population of most levels engaged in these routes is spontaneously depleted before its substantial fraction "leaks" to the thermally activated channels. This applies, for instance, to the pathway activated by excitation at 3000 cm^{-1}, depicted in the left panel of Figure 2.

By and large, the relaxation time exhibits noticeable temperature dependence; elevated temperature tends to temper the dramatic amplitude of the excitation-energy-dependent differences in the temporal behavior (even then, though, their expected scale is at the first glance baffling), while the approximate periodicity of the plot is unaffected.

Combined Effects in Experimental Conditions. In any real experiment, the effects of spectral broadening and temperature-induced reduction of relaxation time variations are inevitably combined. The ensuing graph is shown in Figure 8 (continuous line) for a more or less representative case,

dx.doi.org/10.1021/jp506272b | J. Phys. Chem. A 2014, 118, 9653−9660

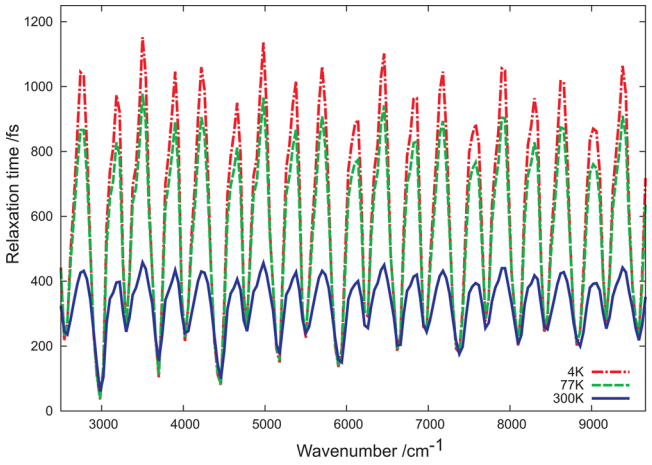

Figure 8. Relaxation time as a function of energy at experimentally relevant temperatures (spectral width, 70 cm^{-1}).

roughly corresponding to the conditions described in ref 14. The relevant experiment was performed at room temperature (here approximated as 300 K), and the fwhm of the autocorrelation trace of the applied gate pulse was 160 fs. For exciting the crystal, this pulse was frequency-doubled, which resulted in a slight temporal broadening, leading to the fwhm of about 200 fs for its cross-correlation with the original gate pulse and suggesting that the intensity autocorrelation function of the exciting light was still somewhat broader. Provided that the spectral width of the pulse was Fourier-transform-limited, it would amount to about 70 cm^{-1} but could be further increased by other factors. Depending on the assumptions in this regard, somewhat different spectral widths are obtained, resulting in the plot blurred to a varying extent.

Qualitatively, the general shape of the calculated energy dependence remains the same as that in the original simplistic picture where no broadening was taken into account, specifically, the relaxation time still varies with energy and the approximate periodicity of these variations is preserved. At 6000 cm^{-1} (here identified with excitation at 3.06 eV in the experiment of ref 14), the calculated relaxation time of about 150 fs agrees nearly perfectly with the experimental result of 120 ± 20 fs. Then, 500 fs observed at 3.20 eV[13] is reasonably represented by the maximum of (a bit over) 400 fs predicted by the calculations at about 7200 cm^{-1}, while the steep decline that follows corresponds to the value of 300−400 fs measured at 3.22 eV.[15] The agreement is practically quantitative, in fact much better than could be expected in view of the simplistic model on which the calculations are based and the fact that no adjustable parameters have been invoked.

Admittedly, owing to equipment factors, the spectral broadening might in reality be larger than assumed here, which would lead to the agreement with experiment deteriorating from excellent to semiquantitative but with a potential for improvements, the latter to be attained by using experimental input frequencies and coupling constants instead of the calculated ones and the density of states upgraded from uniform to energy-dependent. Overall, account taken of the simplistic nature of the adopted model emphasized should be the trends rather than the calculated specific values, and they seem reasonable enough.

The results suggest some new experimental tests. Namely, it might be worthwhile to repeat the measurements of refs 13−15 at lower temperatures. Then, while the fast kinetics reported by Loi et al.[14] at 3.06 eV (about 6000 cm^{-1}) is unlikely to change, the longer relaxation times reported by other authors at specific higher excitation energies are expected yet to increase; liquid nitrogen temperature should be absolutely sufficient to detect a substantial change (broken line in Figure 8). In addition, precise experiments covering the time scale from hundreds to thousands femtoseconds should then reveal the switching of kinetic behavior between single exponential to nonexponential over the excitation energy interval from 7000 to 7300 cm^{-1} (cf. Figure 3).

Such measurements would be highly desirable because the data published to date[13−15] neither support nor refute the hypothesis that the fluorescence rise in 6T may deviate from a single exponential. As a tentative test, we have convoluted the population buildup function $n(t)$ obtained from our calculations for the excitation energy of 6000 cm^{-1} (predicted to be biexponential) with the experimental response function of the apparatus used in the measurements of Loi et al. (cross-correlation signal between the pump pulse going through the sample and the gate pulse).

The result is displayed in Figure 9. The calculated buildup function is compatible with experiment in the sense that it is

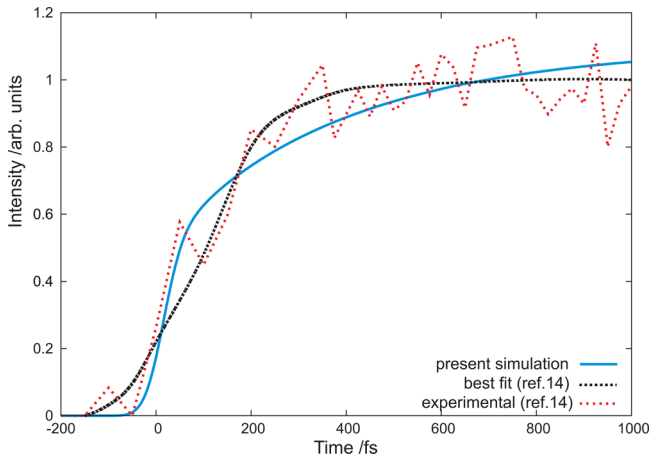

Figure 9. Simulated versus experimental fluorescence buildup in the experiment of ref 14. Dotted lines: raw experimental data and their best fit by Loi et al.; continuous line: our result obtained using the same response function.

contained within the bounds set by the fluctuations in the measured curve, but these are large, which renders the test practically inconclusive because no obvious improvement over the monoexponential fit of Loi et al. is registered. Continuation of the measurements for another 1000 fs would probably clarify the situation as our simulation predicts further emission increase (until the channels depleting the excited-state population become significant) while the single exponential levels off earlier.

DISCUSSION

The model[16] used in the present paper was from the outset aimed primarily at describing the relaxation of high-energy eigenstates deriving from the first Frenkel exciton of the 6T and is indubitably a stark simplification. It entirely ignores the bound exciton−phonon states, prevailing at low excitation energies. This is justified by the fact that, owing to their small radius, the number of bound exciton−phonon states is much smaller than that of their unbound counterparts; moreover,

dx.doi.org/10.1021/jp506272b | J. Phys. Chem. A 2014, 118, 9653−9660

they occur mostly at low energies, while the unbound nature of the high-energy vibronic eigenstates in 6T is confirmed by numerical calculations.[22,23] Effectively, the small spatial overlap between the states belonging to the unbound exciton−phonon continuum (considered in this paper) and the manifold of bound states makes the transition from the former to the latter rather improbable. Accordingly, at high energies where absorption is dominated by the strongly allowed and weakly vibronic-coupled upper Davydov component of the Frenkel state, the role of finite-radius states is generally marginal, both in absorption and in relaxation. Likewise, the intermediate-energy charge-transfer (CT) excitons, crucial in other contexts[24] but consistently disregarded here, are unlikely to participate in the relaxation of high-energy Frenkel excitons, being coupled to the latter only by the overlap-limited (and hence small) CT integrals. Consequently, despite its simplicity, at energies of about 3 eV, the model used here is expected to be valid, with some reservations concerning the uniform density of states that at the quantitative level is not necessarily applicable.

With decreasing excitation energy, the picture is getting less clear because of the increasing contribution from absorption to bound vibronic excitations of Frenkel[25] and CT[24] origin, whose relaxation is certainly dominated by different (intramolecular) mechanisms; for this reason, our plots are not continued to lower energies. Yet, on the basis of the detailed calculations of absorption spectra,[24,25] at least down to about 2.7 eV, the absorption to the exciton−phonon continuum of the upper Davydov component[11,12] (underlying our present estimates) is expected to be significant enough to provide a substantial contribution feeding the emitting state.

Within these limits, our present calculations indicate that the general expectations of the model proposed in the past[16] are supported by numerical solutions of the kinetic equations and are reasonably robust with respect to inevitable experimental limitations. This seems to corroborate the gist of the explanation of the differences in the relaxation times experimentally observed at different excitation energies, provided by the earlier, more idealized, version of the present approach. Presently, the quantitative reproduction of the measured relaxation times legitimizes the underlying theoretical description. At the same time, however, the present results show that the amplitude of previously predicted relaxation time variations[16] is substantially reduced because of temperature broadening, so that the experimentally measured values[13−15] in fact happen to represent the extremes of the expected range. Yet, the variations may be amplified, approximately back to the scale predicted earlier, by performing the measurements at lower temperatures.

The new finding is that, in view of the complex temporal dependence of population buildup in the emitting state, a single value of the fluorescence rise time is not an adequate descriptor of the relaxation process. However, the deviations from monoexponential behavior are expected to be detectable only provided that the measurements, performed at (tens of) femtosecond resolution, are continued in a single run up to the scale of at least several picoseconds.

The predicted earlier[16] quasiperiodic energy-dependent pattern of the relaxation time variations, which by any standards seems a peculiar phenomenon, is now supplemented by the expectation of similar variations in the type of kinetics, embodied in the number of exponentials needed to describe the fluorescence rise. It should be noted in this context that this behavior becomes apparent only on the global scale, that is, if the data are available for a sufficiently long energy interval. Locally, in some parts of the plot, the regularity is far from obvious. When observed in a short energy interval, to an unalerted experimentalist, the seemingly irregular excitation energy dependence is likely to be quite confusing, suggesting equipment failure or other experimental artifacts.

The anticipated seemingly erratic changes of the kinetic regime may look strikingly unusual for a perfectly homogeneous and ordered material. Yet, a qualitatively similar behavior is expected for any organic crystal endowed with an intense upper Davydov component and composed of molecules with multiple vibrational modes coupled to the electronic excitation. In these cases, the methodology presented here may offer some insight into the microscopic mechanisms of the underlying complex relaxation kinetics.

AUTHOR INFORMATION

Corresponding Author

*E-mail: petelenz@chemia.uj.edu.pl.

Notes

The authors declare no competing financial interest.

ACKNOWLEDGMENTS

The authors express their gratitude to Professor M. Loi for illuminating explanations concerning the practice of femtosecond experiments and to Professor J. Najbar for valuable comments. This research was carried out with the equipment purchased thanks to the financial support of the European Regional Development Fund in the framework of the Polish Innovation Economy Operational Program (Contract No. POIG.02.01.00-12-023/08).

REFERENCES

(1) Beddard, G. S.; Fleming, G. R.; Gijzeman, O. L. J.; Porter, G. Vibrational Energy Dependence of Radiationless Conversion in Aromatic Vapours. *Proc. R. Soc. London, Ser. A* **1974**, *340*, 519−533.

(2) Donnelly, M.; Kaufman, F. Fluorescence Lifetime Studies of NO_2. II. Dependence of the Perturbed $^2B_2$ State Lifetimes on Excitation Energy. *J. Chem. Phys.* **1978**, *69*, 1456−1460.

(3) Ramos, R. C.; Fujiwara, T.; Zgierski, M. Z.; Lim, E. C. Photophysics of Aromatic Molecules with Low-Lying $\pi\sigma^*$ States: Excitation-Energy Dependence of Fluorescence in Jet-Cooled Aromatic Nitriles. *J. Phys. Chem. A* **2005**, *109*, 7121−7126.

(4) Mehata, M. S.; Joshi, H. C.; Tripathi, H. B. Edge Excitation Red Shift and Charge Transfer Study of 6-Methoxyquinoline in Polymer Matrices. *J. Lumin.* **2001**, *93*, 275−280.

(5) Wöll, D.; Braeken, E.; Deres, A.; De Schryver, F. C.; Uji-i, H.; Hofkens, J. Polymers and Single Molecule Fluorescence Spectroscopy, What Can We Learn? *Chem. Soc. Rev.* **2009**, *38*, 313−328.

(6) Mollay, B.; Landi, G.; Kauffmann, H. F. Distributed Electronic Relaxation and Nonexponential Fluorescence in Polymers: Reversibility in Donor-Excimer Pairs — A Perturbation Theory Treatment. *J. Chem. Phys.* **1989**, *91*, 3744−3761.

(7) Bodunov, E. N.; Berberan-Santos, M. N.; Martinho, J. M. G. Luminescence Kinetics of Linear Polymer Molecules with Chromophores Randomly Distributed along the Chain. *Opt. Spectrosc.* **2001**, *91*, 694−703.

(8) Kouki, F.; Spearman, P.; Valat, P.; Horowitz, G.; Garnier, F. Experimental Determination of Excitonic Levels in α-Oligothiophenes. *J. Chem. Phys.* **2000**, *113*, 385−391.

(9) Tavazzi, S.; et al. Evidence of Polarized Charge-Transfer Transitions by Probing the Weak Dielectric Tensor Components of Oligothiophene Crystals. *Appl. Surf. Sci.* **2006**, *253*, 296−299.

(10) Fano, U. Effects of Configuration Interaction on Intensities and Phase Shifts. *Phys. Rev.* **1961**, *124*, 1866−1878.

(11) Petelenz, P.; Kulig, W. Unbound Exciton−Phonon States in Oligothiophene Crystals — A Model Approach for Spectroscopic Purposes. *Chem. Phys.* **2008**, *343*, 100−106.
(12) Kulig, W.; Petelenz, P. Spectral Shape of Intense Exciton Absorption in Oligothiophene Crystals. *Phys. Rev. B* **2009**, *79*, 094305.
(13) Frolov, S. V.; Kloc, C.; Batlogg, B.; Wohlgenannt, M.; Jiang, X.; Vardeny, Z. V. Excitation Dynamics in Single Molecular Crystals of α-Hexathiophene from Femtoseconds to Milliseconds. *Phys. Rev. B* **2001**, *63*, 205203.
(14) Loi, M. A.; Mura, A.; Bongiovanni, G.; Cai, Q.; Martin, C.; Chandrasekhar, H. R.; Chandrasekhar, M.; Graupner, W.; Garnier, F. Ultrafast Formation of Nonemissive Species via Intermolecular Interaction in Single Crystals of Conjugated Molecules. *Phys. Rev. Lett.* **2001**, *86*, 732−735.
(15) Cordella, F.; Orru, R.; Loi, M. A.; Mura, A.; Bongiovanni, G. Transient Hot-Phonon-to-Exciton Spectroscopy in Organic Molecular Semiconductors. *Phys. Rev. B* **2003**, *68*, 113203.
(16) Petelenz, P.; Kulig, W. Intraband Relaxation of Frenkel Excitons in Sexithiophene Crystals. *Phys. Rev. B* **2009**, *80*, 115127.
(17) Andrzejak, M.; Pawlikowski, M. Vibronic Effects in the $1^1B_u(1^1B_2)$ Excited Singlet States of Oligothiophenes. Fluorescence Study of the $1^1A_g(1^1A_1) \leftarrow 1^1B_u(1^1B_2)$ Transition in Terms of DFT, TDDFT, and CASSCF Methods. *J. Phys. Chem. A* **2008**, *112*, 13737−13744.
(18) Sumi, H. Theory of Electrical Conduction in Organic Molecular Crystals: Temperature Independent Mobilities. *J. Chem. Phys.* **1979**, *70*, 3775−3786.
(19) Petelenz, P.; Mucha, D. Autoionization of Excited Frenkel States in the Anthracene Crystal. *J. Chem. Phys.* **1994**, *100*, 4607−4614.
(20) Marks, R. N.; Muccini, M.; Lunedi, A.; Michel, R. H.; Murgia, M.; Zamboni, R.; Taliani, C.; Horowitz, G.; Garnier, F.; Hopmeier, M.; Oestrich, M.; Mahrt, F. F. Disorder Influenced Optical Properties of α-Sexithiophene Single Crystals and Thin Evaporated Films. *Chem. Phys.* **1998**, *227*, 49−56.
(21) Sarger, L.; Oberlé, J. How to Measure the Characteristics of Laser Pulses. In *Femtosecond Laser Pulses.* Rullière, C., Ed.; Springer: Berlin, Heidelberg, Germany, New York, 2004.
(22) Stradomska, A.; Petelenz, P. Intermediate Vibronic Coupling in Sexithiophene Crystals. II. Three-Particle Contributions. *J. Chem. Phys.* **2009**, *131*, 044507.
(23) Spano, F. C. Excitons in Conjugated Oligomer Aggregates, Films, and Crystals. *Annu. Rev. Phys. Chem.* **2006**, *57*, 217−24.
(24) Stradomska, A.; Kulig, W.; Slawik, M.; Petelenz, P. Intermediate Vibronic Coupling in Charge Transfer States: Comprehensive Calculation of Electronic Excitations in Sexithiophene Crystal. *J. Chem. Phys.* **2011**, *134*, 224505.
(25) Stradomska, A.; Petelenz, P. Intermediate Vibronic Coupling in Sexithiophene Single Crystals. *J. Chem. Phys.* **2009**, *130*, 094705.